# Riemann surfaces of complex classical trajectories and tunnelling splitting in one-dimensional systems

Hiromitsu Harada, Amaury Mouchet, Akira Shudo

IOP Publishing Journal of Physics A: Mathematical and Theoretical
J. Phys. A: Math. Theor. **50** (2017) 435204 (27pp) https://doi.org/10.1088/1751-8121/aa8c67

# Riemann surfaces of complex classical trajectories and tunnelling splitting in one-dimensional systems

**Hiromitsu Harada**[1], **Amaury Mouchet**[2] **and Akira Shudo**[1]

[1] Department of Physics, Tokyo Metropolitan University, Minami-Osawa, Hachioji, Tokyo 192-0397, Japan
[2] Laboratoire de Mathématiques et de Physique Théorique, Université François Rabelais de Tours—CNRS (UMR 7350), Fédération Denis Poisson, Parc de Grandmont 37200 Tours, France

E-mail: harada-hiromitsu@ed.tmu.ac.jp, shudo@tmu.ac.jp
and Amaury.Mouchet@lmpt.univ-tours.fr

Received 5 May 2017, revised 5 September 2017
Accepted for publication 13 September 2017
Published 4 October 2017


**Abstract**
The topology of complex classical paths is investigated to discuss quantum tunnelling splittings in one-dimensional systems. Here the Hamiltonian is assumed to be given as polynomial functions, so the fundamental group for the Riemann surface provides complete information on the topology of complex paths, which allows us to enumerate all the possible candidates contributing to the semiclassical sum formula for tunnelling splittings. This naturally leads to action relations among classically disjoined regions, revealing entirely non-local nature in the quantization condition. The importance of the proper treatment of Stokes phenomena is also discussed in Hamiltonians in the normal form.

Keywords: tunnelling, fundamental group, complex trajectories, semiclassical analysis

(Some figures may appear in colour only in the online journal)

## 1. Introduction

By definition, tunnelling is a purely quantum effect that cannot be described by any real solution of the classical dynamics. One of the best known signature of it is provided by the splittings in the energy spectrum of a quantum one-dimensional particle in a symmetric double-well potential. A state localised in one well is coupled to its parity-related twin localised in the other well to form a symmetric/antisymmetric doublet of eigenstates delocalised in both wells whose energies differ by a small amount that depends exponentially on the inverse of the Planck constant $\hbar$ or on any classical parameter. Even though no classical real solution

  

connects the two wells, by extending classical dynamics from real to complex plane and applying the WKB method, one can actually capture such nonclassical phenomena. *Instanton* is broadly recognized as a classical path running in the complex plane, which has capability of describing tunnelling in the double-well potential or degenerated vacua in the fields theory [1]. The instanton was originally obtained by performing the so-called Wick rotation of time $t \to \mathrm{i}t$. More generally, one may find in [2–8] some applications of complexifying time in different contexts but the arguments and techniques developed there have mainly been made to understand quantum tunnelling in one dimension.

On the other hand, quantum tunnelling has received renewed interest for these two decades. One driving force for this is that our understanding for classical dynamics has been proceeded considerably and we recognized that qualitative and essential differences in nature of classical dynamics underlie between one and multi-dimensions. In particular, multidimensional systems are known to be nonintegrable in general, which naturally leads to pay attention on the nature of quantum tunnelling in chaotic situations [9–11][3].

There are actually two tasks in performing the semiclassical analysis. The first one concerns how to establish a proper semiclassical formulation providing observed quantities, such as tunnelling splittings. Our second task is to find or even enumerate the inputs—expected to be real or complex classical quantities— which are necessary for the semiclassical analysis.

Concerning formalisms in the semiclassical analysis, if we restrict our interest to energy splittings invoked by quantum tunnelling, explicit and closed formulas are rather limited, although energy splittings are quantities in which tunnelling effects could typically be observed even in experiments. This is the case even in one-dimensional situations [12–15, 20].

The second task would also not be so easy because we need to be thoroughly familiar with classical dynamics in the complex plane. In the case of discrete dynamical systems, fortunately enough, we could make full use of the results gained in recent progress on multidimensional complex dynamical systems and a close link between signatures of quantum tunnelling and complex classical dynamics was discovered [22, 23]. On the other hand, for continuous flow systems, our knowledge about the dynamics in the complex plane is rather fragmental and not enough to reach a unified perspective. Much efforts have been made to explore the nature of singularities in the complex time plane by studying simple scattering models closely [24–26], but the analyses were not exhaustive and remain rather heuristic. This is mainly because the models examined there were still not simple enough in the sense that the nature of singularities appearing in the associated classical dynamics remained too intricated to be handled in a rigorous manner.

Under such circumstances, the aim of the present paper is to focus on the second issue and establish models which allow full enumeration of complex orbits necessary for the semiclassical analysis of tunnelling splittings. This will be achieved for the systems whose Hamiltonians

[3] **Notes** We should also mention that there is an abundant literature on these matters in mathematical physics. Two lines of thought may be identified (i) the first one, initiated by Harrell [41] for the quartic 1d-potential, relies on instantons, that were later seen as geodesics for a measure, called the Agmon measure, that evaluates the quantity of 'classical interdiction'. The extension to multidimensional systems was made by Davies [42, theorem 4] (exponential majoration), then by Simon [43, theorem 1] (exponential behaviour), Helffer and Sjöstrand [45, 47, 48] (prefactor of the exponential). (ii) The second school plays also with the exponential behaviour of the wavefunctions outside the wells but by directly complexifying the time in the Schrödinger equation and then applying the semiclassical methods developed by Maslov [49, 50]. These two schools are mainly concerned by the tunnelling doublet of lowest energy (see however [52]) and surprisingly enough the authors seem to consider as secondary the crucial hypothesis that allows to explain the dichotomy between tunnelling in integrable and non-integrable systems. This hypothesis is let implicit in [43] (one has to isolate the Agmon geodesics, see condition (1.1) of theorem (1.1) in [51], this hypothesis is not even mentioned in theorem 1.5 of [44] and appears indirectly in [46] through the hypothesis of the non degeneracy of the instanton trajectories, see also section 4, hypothesis $H_4$ in [53]) and we were not even able to identify it in the work of the Russian school.

are given as polynomial functions. If Hamiltonian functions are polynomial, any local classical quantities are algebraic functions of the dynamical variables, which greatly simplifies the Riemann sheet structure and makes it possible to develop rigorous arguments on classical dynamics in the complex plane. In particular, because there is a finite number of algebraic singularities and no essential singularities, we can easily describe the associated Riemann surface and its fundamental group.

The organization of the present paper is as follows. In section 2, we introduce the semiclassical formula for tunnelling splittings which was derived in [15]. Our argument will throughout be based on it. We also mention the limitation of our analysis, especially in view of the Stokes phenomenon. Section 3 is devoted to explaining our strategy to enumerate topologically distinct complex paths. A key idea is to examine the fundamental group of the Riemann surface for the associated function, which makes it possible to obtain a complete list complex paths. In sections 4 and 5, simple models, one-dimensional systems with double- and triple-well potentials, are recast with special focus on the method of listing the relevant complex paths we introduced in section 3. An advantage in taking such an approach is that one can find non-trivial global relations among action integrals appearing in the semiclassical formula. In section 6, we show that such action relations imply a sufficient condition under which distinct potential wells are simultaneously quantized. Since the condition originates only from the global topology of the Riemann surface, the argument applies even in asymmetric multi-well potential systems. In section 7, we apply our fundamental-group-based inventory to a richer integrable model constructed with the help of Hamiltonian normal forms. However, in section 8, we emphasize that handling of the Stokes phenomenon done in the cases of double- and triple-well models are improper for the normal form Hamiltonian model by showing a counterexample for which a naive prescription in dealing with the Stokes phenomenon does not work.

## 2. Semiclassical formula for the tunnelling splitting

In this section, we introduce a semiclassical formula on which we will rely throughout the following analysis for tunnelling splitting in multi-well potential and normal form Hamiltonian systems. In [15], a semiclassical trace formula for tunnelling splittings has been derived and it was shown to work well in predicting tunnelling splittings for a symmetric triple-well potential system. Below we briefly explain the formula to show how *complex classical orbits* come into play in determining tunnelling splittings (see more details in appendix A and [15]).

Let us consider a one-dimensional constant classical Hamiltonian $H(p,q)$ having reflection symmetry with respect to the canonical variables $p$ and $q$:

$$H(p,q) = H(-p,-q). \tag{1}$$

The energies $E_n^{\pm}$ and the associated eigenstates $|\phi_n^{\pm}\rangle$ of the corresponding quantum model are given by

$$\hat{H}|\phi_n^{\pm}\rangle = E_n^{\pm}|\phi_n^{\pm}\rangle, \tag{2}$$

where $\hat{H} \stackrel{\text{def}}{=} H(\hat{p},\hat{q})$ with $\hat{p}$ and $\hat{q}$ being the canonical operators associated with $p$ and $q$ respectively. The superscripts $\pm$ stand for the symmetric/antisymmetric states and tunnelling is manifest through the splittings $\Delta E_n \stackrel{\text{def}}{=} E_n^- - E_n^+$.

In [15], a semiclassical formula for the energy splitting $\Delta E_n$ has been derived as

$$\Delta E_n \sim \frac{\hbar}{2T}\sum_{\text{cl}}(-1)^{\mu+1}\mathrm{e}^{\mathrm{i}S_{\text{cl}}/\hbar}, \tag{3}$$

where the sum is taken over all the classical paths with energy $E \sim E_n^{\pm}$ such that $q(T) = -q(0)$ and $p(T) = -p(0)$ for a given time interval $T$. Although the time interval $T$ appears explicitly in the formula, it has been shown in [15] that the right-hand side of (3) becomes independent of $T$ as long as $\mathrm{Im}\, T$ is taken to be large enough compared to the typical (real) period of the classical system.

The quantities $S_{\mathrm{cl}}$ and $\mu$ denote the classical action of path $\Gamma$

$$S_{\mathrm{cl}} = \int_{\Gamma} p(q)\mathrm{d}q, \tag{4}$$

and the Maslov index [16], respectively. The function $p(q)$ is defined by

$$H(p, q) = E \tag{5}$$

where $E \simeq E_n^{\pm}$ and we will always left implicit the dependence on $E$. Since there exist no real classical paths connecting two classically disjointed regions, the path $\Gamma$ runs in the complex plane.

Formula (3) comes from the saddle point approximation therefore, in order to apply it, two steps can be identified. The first one is to list all the possible complex paths that could contribute to the sum in the formula and the second step is to select in this list of candidates those that actually contribute to $\Delta E_n$. As far as the first step is concerned, in general, even in the simplest models such as double-well potential systems, the classical solutions with appropriate boundary conditions occur in families of infinite numbers and it is a non-trivial task to enumerate all these stationary paths. Even after enumerating all the possible candidates, it is known that not all of them do not necessarily remain as final contributions. This is because the Stokes phenomenon occurs in the complex plane, and some saddles have to be excluded from the final contribution. The second step we should consider is therefore to find a proper way of handling the Stokes phenomenon.

In [15], the formula (3) was satisfactorily tested in some standard models with a procedure for achieving the first step that does not guarantee that all the possible complex stationary path were considered. To justify the adopted method and to have a better control on the approximations, we need to establish a systematic way, based on more rigorous grounds, to achieve step one. Our subsequent argument will be focused mainly on this step. Concerning the second step, although the Stokes phenomenon could be now captured as a well recognized object [17–19] and even within the scope of rigorous arguments thanks to recent progress of the so-called *exact WKB analysis*, or *resurgent theory* [27], we will not take into account the Stokes phenomenon based on such recent developments, rather treat the Stokes phenomenon in a heuristic way, as explained below.

As is easily seen, classical actions associated with complex paths have imaginary parts, and the complex path(s) with the most dominant weight are supposed to have minimal imaginary action. Note that such an argument of course holds only after handling the Stokes phenomenon in an appropriate manner. Our task here is therefore to enumerate all the possible candidate complex paths and then to specify the complex path with the smallest imaginary action out of the candidates.

The strategy for the first step is to examine the *fundamental group* of the Riemann surface $R$ of the function $p(q)$ since the fundamental group provides the topological independent paths on a given surface. In addition to such information we also need to specify singularities of the function $p(q)$. This is because, by virtue of Cauchy theorem, the value of the classical action (4) is affected when a continuous deformation of $\Gamma$ crosses singularities.

## 3. Fundamental group of Riemann surfaces of algebraic functions

In this section, we show how the fundamental group of the Riemann surface $R$ of the function $p(q)$ helps to construct the path $\Gamma$ along which the classical action (4) is computed. In what follows, we assume that our Hamiltonian $H(p,q)$ is expressed as a polynomial function of $p$ and $q$ and the polynomial is irreducible. The former condition allows to obtain the complete list of the complex paths contributing to the semiclassical sum (3) and the latter condition ensures that the Riemann surface of the function $p(q)$ is connected.

$H$ being a polynomial, the function $p(q)$ defined by (5) is an algebraic function and therefore has at most finitely many singularities [28] that are points where $p(q)$ has a pole or a branch cut. Since our Riemann surface $R$ is constructed from an algebraic function and assumed to be irreducible, it is homeomorphic to a surface of a finite genus $g$, or $g$-fold torus for short, accompanied with finite number of holes associated with singularities of the function under consideration. The genus of the surface is given by the formula $g = w/2 - d + 1$, where $w$ is the ramification index and $d$ is the highest degree of $p$ in the polynomial in question. Especially, $w$ is equal to the number of branch points if all branch points are square-root type, i.e. the function is double-valued near each branch point. For example, in multi-well potential systems discussed in sections 4 and 5, and the normal form Hamiltonian system in section 7 as well, $p(q)$ is shown to be double-valued functions near each branch point.

The fundamental group on the Riemann surface is introduced as the group whose elements are identified through homotopy equivalence of curves on the surface. For the $g$-fold torus, there exist $2g$ independent homotopically equivalent loops, and following the convention we call the half of them $\alpha_i$-loop and the rest $\beta_i$-loop ($1 \leqslant i \leqslant g$). The loops $\alpha_i$ and $\beta_i$ are often called *homology basis* in the literature [28].

When computing (4) one must include the contribution of singularities which could provid non-zero residues, when by deforming $\Gamma$. This means that the associated fundamental group should be replaced by the one incorporating singularities of the function $p(q)$. The Seifert–van Kampen theorem tells us that the fundamental group for a surface with holes is obtained as the product of the fundamental group for the original $g$-fold torus and that of a sphere with $m$ holes, where $m$ is the number of holes [29], which appear as either poles or branch points in the present situation. We call the loop encircling a hole the $\gamma_i$ loop ($1 \leqslant i \leqslant m$), again following the convention. The loop $\gamma_i$ here is taken to be a small closed loop around each hole (see figure 1).

We note also from the Seifert–van Kampen theorem that the elements $\alpha_i, \beta_i$ and $\gamma_i$ of the fundamental group satisfy a relation,

$$\prod_i \alpha_i \beta_i \alpha_i^{-1} \beta_i^{-1} = \prod_i \gamma_i \tag{6}$$

implying that all the loops $\alpha_i, \beta_i$ and $\gamma_i$ are not independent with each other. We hereafter assume that one of $\gamma_i$-loops, say $\gamma_m$, is expressed in terms of the other loops. We just graphically show in figure 1 why the relation (6) follows in the simplest situation where a simple torus with $g = 1$ is connected with a sphere with with a hole.

Using the elements of the fundamental group, we can now enumerate all the topologically distinct paths obtained from a reference path $\Gamma_0$. More concretely, for an arbitrarily chosen reference path $\Gamma_0$ with fixed initial and final ends in the $q$-plane, topologically independent paths associated with the reference path $\Gamma_0$ are expressed as

$$\Gamma = \Gamma_0 + \sum_{i=1}^{g} n_{\alpha_i} \alpha_i + \sum_{i=1}^{g} n_{\beta_i} \beta_i + \sum_{i=1}^{m-1} n_{\gamma_i} \gamma_i, \tag{7}$$

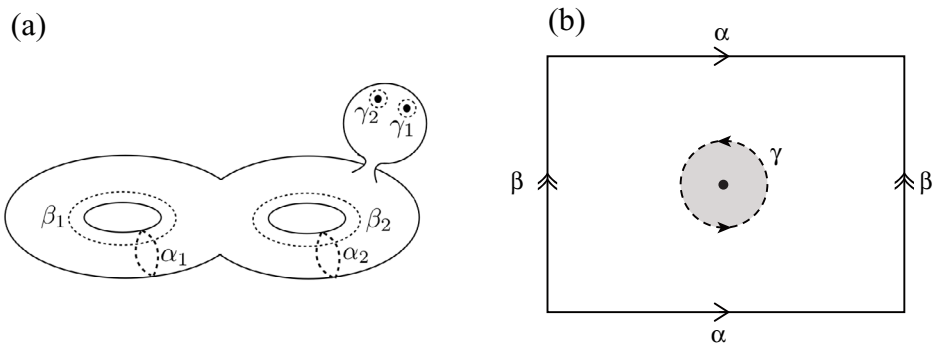


**Figure 1.** (a) An example of the Riemann surface. Here the case for the 2-fold torus with two holes is presented. Homology bases of the fundamental group are shown as $\alpha_1, \alpha_2, \beta_1, \beta_2, \gamma_1$ and $\gamma_2$. (b) A graphical proof for the relation (6). A simple torus with a hole is here assumed.

where $n_{\alpha_i}, n_{\beta_i}$ and $n_{\gamma_i}$ are integers and will be called winding numbers. In what follows we apply the scheme formulated in this way to a couple of concrete examples, some of them are the systems already well studied.

## 4. Double-well potential case

As a simple example, we first discuss a double-well potential system:

$$H(p,q) = \frac{p^2}{2} + V(q), \tag{8}$$

$$V(q) = E + (q-q_1)(q-q_2)(q-q_3)(q-q_4). \tag{9}$$

Here $q_i$ $(1 \leqslant i \leqslant 4)$ are real parameters satisfying $q_1 < q_2 < q_3 < q_4$ and $E$ is the total energy. We further assume that the potential function is symmetric, that is $q_1 = -q_4, q_2 = -q_3$ (see figure 2) in accordance with (1) eventhough this symmetry condition is not relevant for topological considerations. From (5) we find

$$p(q) = \pm\sqrt{-2(q-q_1)(q-q_2)(q-q_3)(q-q_4)}. \tag{10}$$

The function $p(q)$ has four branch points at $q = q_i$ $(1 \leqslant i \leqslant 4)$, which are all located on the real axis and one can choose the intervals $[q_1, q_2]$ and $[q_3, q_4]$ as two cuts defining a Riemann surface with two leaves. As shown in figure 3, we project each leaf onto the Riemann sphere and continuously deform two spheres by opening the branch cuts. We finally get a simple torus with $g = 1$ with holes associated with the singularities.

The homology basis of the fundamental group in this case is composed of $\alpha, \beta$, which are homotopically independent loops on the torus, together with the loops encircling singularities. In addition to branch points at $q = q_i$ $(1 \leqslant i \leqslant 4)$, there exist poles at $q = \pm\infty$, and we denote the loops associated with singularities by $\gamma_i$ $(1 \leqslant i \leqslant 4)$ and $\gamma^{(\pm\infty)}$, respectively (see figure 4). Relations (6) allow to express, $\gamma_4$, say, as a product of the other loops considered to be independent. As shown in the previous section, with fixed initial and final end points, the variety of distinct values of the action integral is given based on the formula (7).

Recall the semiclassical formula (3) for the tunnelling splitting requires the complex paths connecting the points symmetrically located in the $q$-plane then we may take $\Gamma_0$ to connect $q_2$

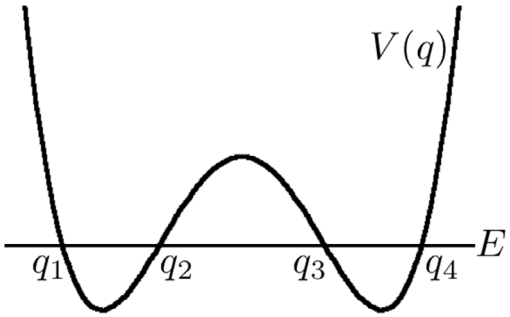


**Figure 2.** The double-well potential $V(q)$.

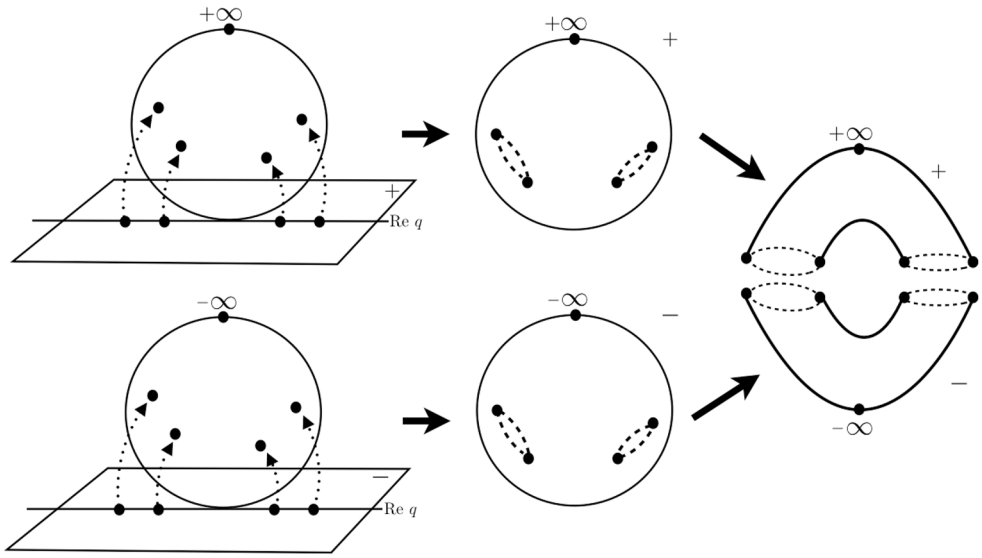


**Figure 3.** Deformation of Riemann spheres to a torus is shown in the double-well potential case. The black dots and the dashed lines represent branch points and branch cuts, respectively. $\pm$ signs show the branches of $p(q)$.

and $q_3 = -q_2$. Without loss of generality, we can obtain arbitrary symmetric paths from the path connecting the branch points $q_2$ and $q_3$ by shifting both initial and final points simultaneously keeping the symmetry condition. All the topologically distinct paths, taking into account the contribution from divergent singularities, are then written as

$$\Gamma = \Gamma_0 + n_\alpha \alpha + n_\beta \beta + \sum_{i=1}^{3} n_{\gamma_i} \gamma_i + n^{(+\infty)} \gamma^{(+\infty)} + n^{(-\infty)} \gamma^{(-\infty)}, \tag{11}$$

where $n_\alpha, n_\beta, n_{\gamma_i}$ and $n^{(\pm\infty)}$ are winding numbers of each loop.

As is discussed below, it is important to specify the $\alpha$ and $\beta$ loops explicitly when one actually evaluates the action integrals, while we can freely move and deform the $\alpha$ and $\beta$ loops and the locations are not relevant within the argument of the fundamental group (see figure 1).

For simplicity, we take two independent loops $\alpha$ and $\beta$ on the torus in such a way that each branch in the $\alpha$ loop runs along the real $q$-axis with encircling the two branch points $q_1$ and

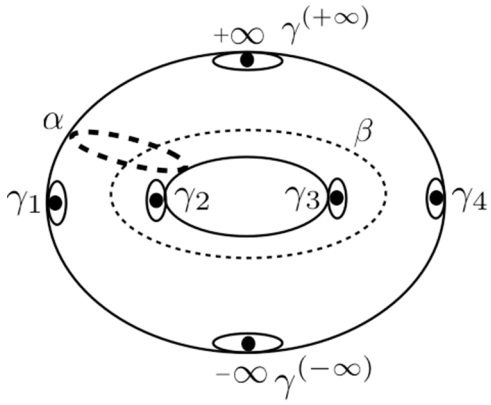


**Figure 4.** Homology basis of the fundamental group for the torus $\mathcal{T} \setminus \{q_1, q_2, q_3, q_4, +\infty, -\infty\}$.

$q_2$, and in the same way the $\beta$ loop encircles the two branch points $q_2$ and $q_3$ (see figure 5). By taking the loops $\alpha$ and $\beta$ in this manner, the action integral for the $\alpha$ loop turns out to be real valued and that for the $\beta$ loop purely imaginary valued. As shown in appendix B, the action integrals for $\gamma_i$ $(i = 1, 2, 3)$ vanish. We then reach the expression for the total action integral after summing over all the contributions as

$$S_\Gamma = S_{\Gamma_0} + n_\alpha S_\alpha + n_\beta S_\beta + n^{(+\infty)} S^{(+\infty)} + n^{(-\infty)} S^{(-\infty)}, \tag{12}$$

where

$$\begin{aligned} S_{\Gamma_0} &:= \int_{q_2}^{q_3} p\mathrm{d}q, \\ S_\alpha &:= \oint_\alpha p(q)\mathrm{d}q = 2\int_{q_1}^{q_2} p\mathrm{d}q, \\ S_\beta &:= \oint_\beta p(q)\mathrm{d}q = 2\int_{q_2}^{q_3} p\mathrm{d}q, \\ S^{(\pm\infty)} &:= \oint_{\gamma^{(\pm\infty)}} p(q)\mathrm{d}q. \end{aligned} \tag{13}$$

Now we show that $S_\alpha$ and $S^{(\pm\infty)}$ are not independent and actually related with each other. To see this, we rewrite as $S_L = S_\alpha$ for left-side well, and introduce the action integral for the right-side well as

$$S_R = 2\int_{q_3}^{q_4} p\mathrm{d}q. \tag{14}$$

As illustrated in figure 6, the integration contour specifying the action integral $S_L$ is continuously deformed and split into the ones associated with the action integrals $S^{(+\infty)}$ and $S_R$. This leads to the relation

$$S_L = S_R - S^{(+\infty)}, \tag{15}$$

where the minus sign in front of $S^{(+\infty)}$ comes from the phase of $p$ (see appendix C). From the symmetry of the potential function, it is obvious that $S_L = S_R$ holds. This automatically gives $S^{(+\infty)} = 0$, which can also be confirmed by the direct calculation of the residue at $q = +\infty$

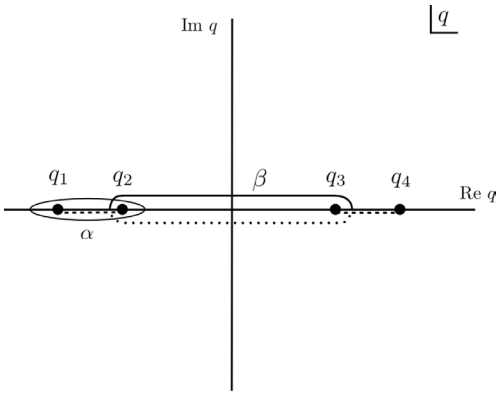


**Figure 5.** $\alpha, \beta$ loops taken as integration contours on the $q$ plane.

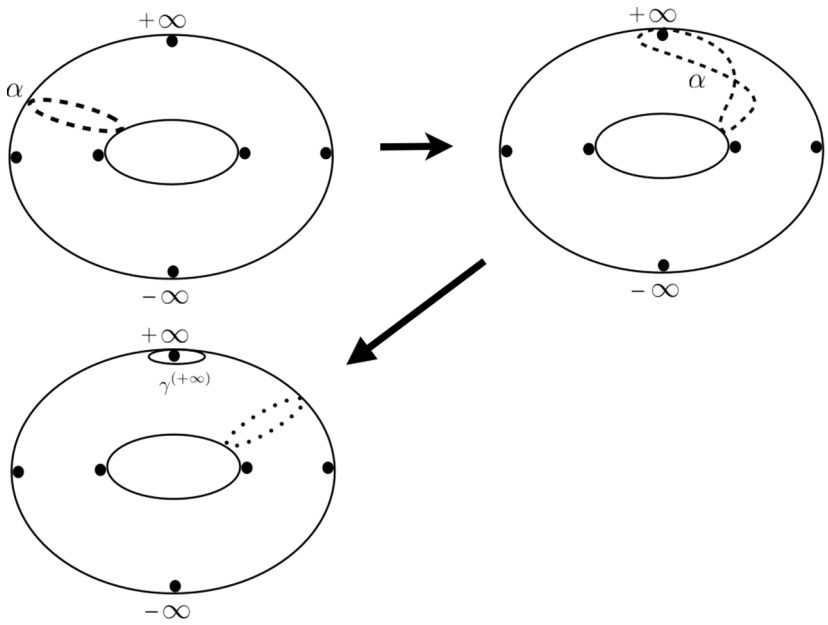


**Figure 6.** Deformation of the $\alpha$ loop in the left well. It splits into a combination of the $\alpha$ loop in the right well and a loop around $+\infty$.

(also see appendix C). From this observation, the candidates of action integrals finally take a simple form as

$$S_\Gamma = S_{\Gamma_0} + n_\alpha S_\alpha + n_\beta S_\beta. \tag{16}$$

Next we turn our attention to the most dominant complex path in the semiclassical formula (3). Since classical action integrals under consideration are complex valued, the most dominant contribution is supposed to come from the complex classical orbit(s) with minimal imaginary action $\mathrm{Im}\, S$. In the present situation, the $\alpha$ loop contribution is real valued, so the imaginary part of action integral is written as

$$\mathrm{Im}\, S_\Gamma = \mathrm{Im}\, S_{\Gamma_0} + n_\beta \mathrm{Im}\, S_\beta. \tag{17}$$

This may take arbitrarily large negative values as $n_\beta$ is allowed to be any integer, positive or negative, meaning that imaginary action can become arbitrarily small. However, it is obvious that the orbits with negative imaginary action give rise to exponentially large contributions, which are not physically accepted, so should be dropped from the final contributions.

Excluding unphysical contributions out of necessary ones could be done by handling the Stokes phenomenon properly. This would therefore be a matter of issues which should be closely discussed in order to make our theory self-consistent. However, as mentioned in section 2, we here treat the Stokes phenomenon only in a heuristic manner. The principle we adopt is based on the behavior of imaginary action as time proceeds. From the Hamiltonian equations of motion, $\mathrm{d}q = p\mathrm{d}t$ follows, which results in $\int p\mathrm{d}q = \int p^2\mathrm{d}t$. We then have

$$\mathrm{Im}\, S = \int -\mathrm{Im}\, p^2 \mathrm{Im}\, \mathrm{d}t. \tag{18}$$

and in order to get $\mathrm{Im}S > 0$ we will choose a parametrisation such that $\mathrm{Im}\, \mathrm{d}t < 0$. In this choice, $\mathrm{Im}\, S$ becomes negatively large with increase in $\mathrm{Im}\, \mathrm{d}t$ in a monotonic way.

If one applies this rule, which will also be used in the examples discussed below, $\Gamma_0$ is given as a trajectory passing through the potential barrier only once, that is a half cycle of the $\beta$ loop, and the smallest imaginary action is just

$$\mathrm{Im}\, S_\Gamma = \frac{1}{2} S_\beta. \tag{19}$$

This is nothing but the imaginary action for the so-called instanton path. From the expression (16), the corresponding real part turns out to be

$$\mathrm{Re}\, S_\Gamma = n_\alpha S_\alpha. \tag{20}$$

Since branch points are turning points and $\alpha$, $\beta$ loops encircle the two branch points, we find that the Maslov index is equal to $\mu = 2n_\alpha + 1$. Incorporating the semiclassical quantization condition $S_\alpha = (1/2 + N)2\pi\hbar$, the formula (3) can now be explicitly written as

$$\frac{\hbar}{2T} \mathrm{e}^{-S_\beta/2\hbar} \sum_{n_\alpha} (-1)^{2n_\alpha+2} (-1)^{n_\alpha}. \tag{21}$$

Here the sum over the winding number $n_\alpha$ is canceled except for the case $n_\alpha = 0$. From these arguments we finally obtain the formula

$$\Delta E \sim \frac{\hbar}{2T} \mathrm{e}^{-S_\beta/2\hbar}. \tag{22}$$

This is nothing but the well known formula in the instanton theory, and also coincides with the result rederived in [15].

## 5. Triple-well potential case

As a next example, we consider a triple-well potential system:

$$H(p,q) = \frac{p^2}{2} + V(q), \tag{23}$$

$$V(q) = E + (q-q_1)(q-q_2)(q-q_3)(q-q_4)(q-q_5)(q-q_6),$$

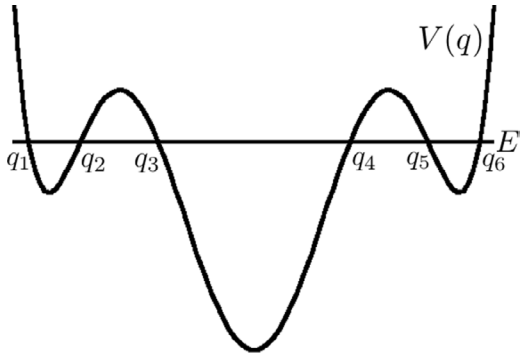


**Figure 7.** The triple-well potential $V(q)$.

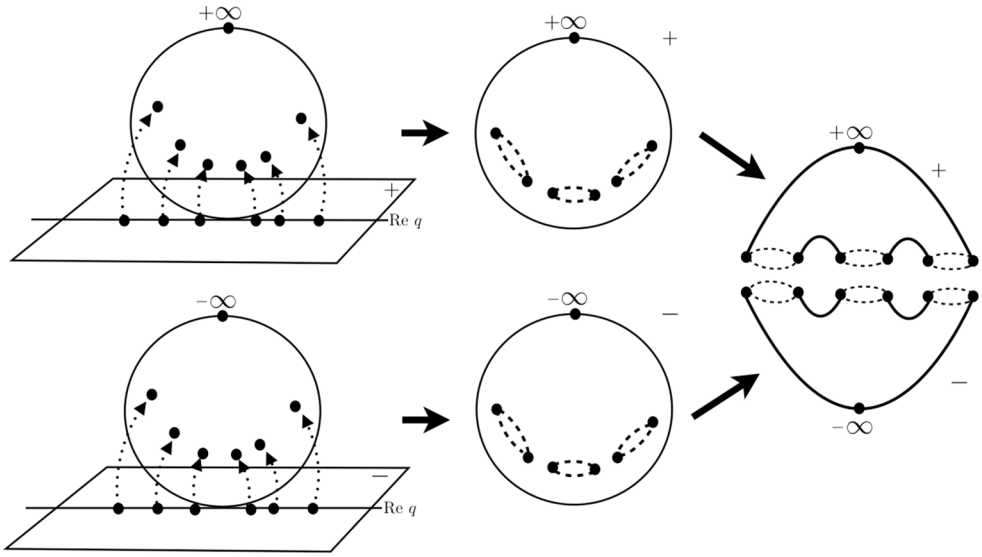


**Figure 8.** Deformation of Riemann spheres to a torus is shown in the triple-well potential case. The black dots and the dashed lines represent branch points and branch cuts, respectively. $\pm$ signs show the branches of $p(q)$.

where the parameters $q_i$ $(1 \leqslant i \leqslant 6)$ are all real and satisfy the conditions $q_1 < q_2 < \cdots < q_6$. We again assume the conditions $q_1 = -q_6, q_2 = -q_5, q_3 = -q_4$ in order to develop the semi-classical analysis for the tunnelling splitting (see figure 7).

In the same way as the double-well case, we obtain $p(q)$ as

$$p(q) = \sqrt{-2(q-q_1)(q-q_2)(q-q_3)(q-q_4)(q-q_5)(q-q_6)}.$$

The function $p(q)$ has now six branch points on the real axis. The associated Riemann surface of $p(q)$ is homeomorphic to a 2-fold torus with small holes associated with branch points and poles (see figure 8). The homology basis of the fundamental group is composed of the loops $\alpha_i$ and $\beta_i$ $(i = 1, 2)$ on the 2-fold torus and $\gamma_i$ $(1 \leqslant i \leqslant 6)$ and $\gamma^{(\pm\infty)}$, each of which is a small loop encircling the corresponding singularity. We illustrate in figure 9 the elements of the fundamental group in this case.

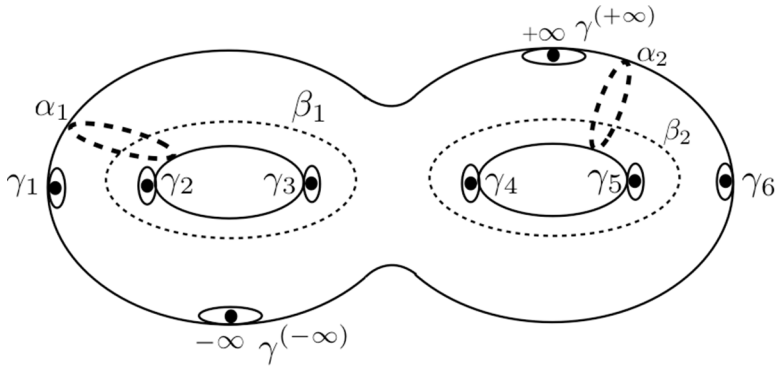


**Figure 9.** Homology basis for the surface $\mathcal{T}\#\mathcal{T} \setminus \{q_1, q_2, q_3, q_4, q_5, q_6, +\infty, -\infty\}$.

To discuss the tunnelling splitting between the states localized at the left- and right-wells, let $\Gamma_0$ be a path connecting the branch points $q_2$ and $q_5 = -q_2$. The integration contour is given by a combination of these loops as follows, keeping in mind that $\gamma_6$ is a product of the other loops,

$$\Gamma = \Gamma_0 + \sum_{i=1}^{2} n_{\alpha_i}\alpha_i + \sum_{i=1}^{2} n_{\beta_i}\beta_i + \sum_{i=1}^{5} n_{\gamma_i}\gamma_i + n^{(+\infty)}\gamma^{(+\infty)} + n^{(-\infty)}\gamma^{(-\infty)}, \tag{24}$$

where $n_\alpha, n_\beta, n_{\gamma_i}$ and $n^{(\pm\infty)}$ are winding numbers of each loop. Again using the result shown in appendix B, the action integrals for $\gamma_i$ $(i = 1, 2, \cdots, 5)$ all vanish, and we reach the expression for the total action integral contributions,

$$S_\Gamma = S_{\Gamma_0} + \sum_{i=1}^{2} n_{\alpha_i} S_{\alpha_i} + \sum_{i=1}^{2} n_{\beta_i} S_{\beta_i} + n^{(+\infty)} S^{(+\infty)} + n^{(-\infty)} S^{(-\infty)}, \tag{25}$$

where

$$\begin{aligned}
S_{\Gamma_0} &:= \int_{q_2}^{q_5} p\mathrm{d}q, \\
S_{\alpha_1} &:= \oint_{\alpha_1} p\mathrm{d}q = 2\int_{q_1}^{q_2} p\mathrm{d}q, \\
S_{\alpha_2} &:= \oint_{\alpha_2} p\mathrm{d}q = 2\int_{q_5}^{q_6} p\mathrm{d}q, \\
S_{\beta_1} &:= \oint_{\beta_1} p\mathrm{d}q = 2\int_{q_2}^{q_3} p\mathrm{d}q, \\
S_{\beta_2} &:= \oint_{\beta_2} p\mathrm{d}q = 2\int_{q_4}^{q_5} p\mathrm{d}q, \\
S^{(\pm\infty)} &:= \oint_{\gamma^{(\pm\infty)}} p(q)\mathrm{d}q.
\end{aligned} \tag{26}$$

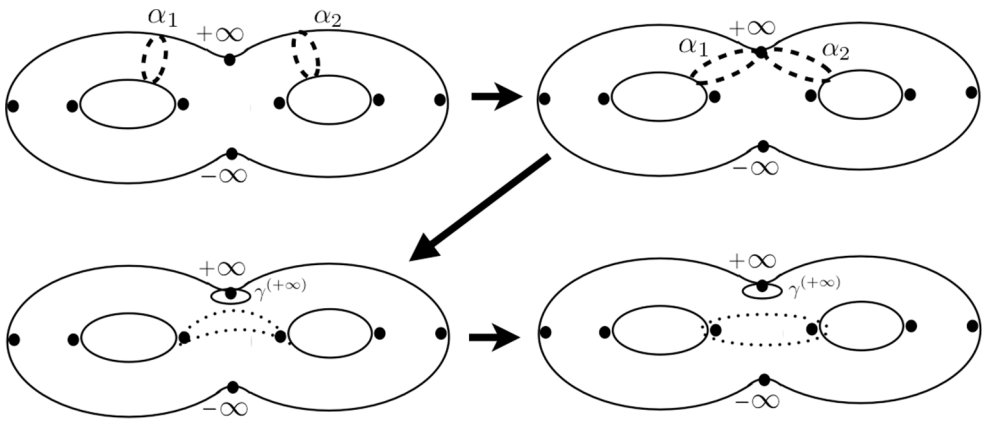


**Figure 10.** Deformation of the $\alpha_1$ and $\alpha_2$ loops in the left- and right-wells. They split into a combination of the loop for the central well and a loop encircling $+\infty$.

As done in the double well potential case, we next show that these action integrals are not independent. As illustrated in figure 10, the integration contours specifying $S_{\alpha_1}$ and $S_{\alpha_2}$ are continuously deformed and split into the ones associated with the action integrals $S^{(+\infty)}$ and $S_C$. Here $S_C$ stands for the action integral for the central well,

$$S_C := 2\int_{q_3}^{q_4} p\mathrm{d}q. \tag{27}$$

Rewriting the notation as $S_L = S_{\alpha_1}$ and $S_R = S_{\alpha_2}$ to make clear that $S_{\alpha_1}$ and $S_{\alpha_2}$ are action integrals for the left- and right-side wells, we obtain the relation

$$S_C = S_L + S_R + S^{(+\infty)}. \tag{28}$$

This relation can also be confirmed in the direct calculation presented in appendix C. A similar relation holds for $S^{(-\infty)}$ except that the sign in front of $S^{(-\infty)}$ is minus.

The symmetry of the potential function leads to the relations $S_R = S_L$, and $S_{\beta_1} = S_{\beta_2}$. As a result, all the possible classical action integrals are simply expressed as

$$S_\Gamma = S_{\Gamma_0} + n_L S_L + n_C S_C + (n_{\beta_1} + n_{\beta_2}) S_{\beta_1}. \tag{29}$$

Note that the winding numbers are introduced as $n_L := n_{\alpha_1} + n_{\alpha_2} - 2n_C$ and $n_C := n^{(+\infty)} - n^{(-\infty)}$.

The principle to incorporate the Stokes phenomenon is the same as before. The imaginary part of complex paths is written as

$$\mathrm{Im}\, S_\Gamma = \mathrm{Im}\, S_{\Gamma_0} + (n_{\beta_1} + n_{\beta_2})\mathrm{Im}\, S_{\beta_1}, \tag{30}$$

and we require that the imaginary component of time $t$ is decreasing. Under this condition, the complex path with the minimal imaginary action is given as the one with $n_{\beta_1} = n_{\beta_2} = 0$. The corresponding orbit starts from the left-side well and crosses over two potential barriers and reaches the right-side well. The resulting imaginary action is evaluated twice as much as the instanton action in each barrier:

$$\mathrm{Im}\, S_\Gamma = \mathrm{Im}\, S_{\beta_1}. \tag{31}$$

Concerning the real part of the action integral, the path $\Gamma$ has to go half round the central well, so the real part of the action is given as

$$\mathrm{Re}\, S_\Gamma = n_L S_L + (n_C + \frac{1}{2}) S_C, \tag{32}$$

and the Maslov index is also evaluated similarly to give $\mu = 2n_L + 2n_C + 3$. We finally get the semiclassical expression for the tunnelling splitting:

$$\Delta E_n \sim \frac{\hbar}{2T} \mathrm{e}^{-S_{\beta_1}/\hbar} \sum_{n_L, n_C} (-1)^{\mu+1} \mathrm{e}^{\mathrm{i}(n_L S_L + (n_C + \frac{1}{2}) S_C)/\hbar}. \tag{33}$$

This almost coincides with the formula derived in [15], but the way of enumerating the paths differs from the one adopted there, so the form of the sum is slightly different. As also discussed in [15], the interference caused by the sum in the right-hand side gives rise to resonances, which generate a series of spikes in the $\Delta E$ versus $1/\hbar$-plot. Such a phenomenon could be understood as the resonant tunnelling or the Fabry–Pérot effect in optics [30, 31].

## 6. Simultaneous quantization

As given in (15) and (28) the action integrals for the $\alpha$ loops in the fundamental group are related through the action integral associated with the loop encircling infinity. These relations will invoke *simultaneous quantization* of distinct wells. Simultaneous quantization in distinct wells has been discussed in [32], and the result obtained above is essentially the same as the one derived there in the double-well potential case.

We first explain how simultaneous quantization is achieved in the double-well case. Suppose the action integral for the left-side well is quantized as $S_L = (1/2 + m_L)2\pi\hbar$. From the relation (15), the action for the right well is also quantized as $S_R = (1/2 + m_R)2\pi\hbar$ if and only if the action integral around infinity satisfies the condition $S^{(\infty)} = 2\pi\hbar m^{(\infty)}$, where $m_R, m_L$ and $m^{(\infty)}$ are integers.

Concerning the triple-well system, the relation (28) among action integrals is not enough to give simultaneously quantization of $S_L$ and $S_R$ even if $S^{(\infty)} = 2\pi\hbar m^{(\infty)}$ with integers $m^{(\infty)}$ is satisfied. However, if the potential is symmetric as assumed in section 5, $S_L$ and $S_R$ are quantized simultaneously since $S_L = S_R$ follow in such a case.

Note that the relations (15) and (28) hold among the $\alpha$ loops in the fundamental group. It would be natural to explore whether or not the relation involving $\beta$ loops exist, which might provide further constraints for action integrals. Integrals of algebraic functions along $\alpha$ or $\beta$ loops are called periods of Abelian integrals [28]. In a general argument of Abelian integrals, the period of Abelian integrals of the first kind has a relation as

$$\left( \int_{\beta_1} \omega, \cdots, \int_{\beta_g} \omega \right) = \left( \int_{\alpha_1} \omega, \cdots, \int_{\alpha_g} \omega \right) T, \tag{34}$$

where $T$ is called the period matrix and $\omega$ is the Abelian differential of the first kind, respectively [33]. However, since the function $p(q)$ has poles in the Riemann surface, the relation among $\alpha$ or $\beta$ loops might not take a linear form as given in (34). If the relation is linear, it would not provide an additional relation generating extra constraints concerning the quantization condition.

## 7. Normal form hamiltonian

In this section, we examine the case where the Hamiltonian is built from more general normal forms and whose tunnelling splittings were semiclassically studied in [20] in order to

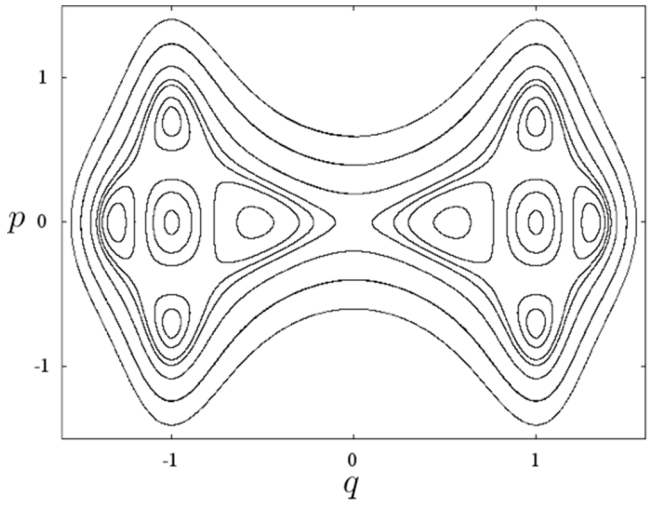


**Figure 11.** Equi-energy contours for the Hamiltonian (36).

investigate the validity of the so-called resonance-assisted tunnelling scenario (RAT) [21, 34]. As shown below, equi-energy contours look like typical patterns observed in the Poincaré section of phase space in two-dimensional nearly integrable systems. With a Hamiltonian of the form [35]

$$H(p,q) = \sum_{k=1}^{n} a_k (p^2+q^2)^k + \sum_{l,m} b_{l,m} q^l p^m, \tag{35}$$

where $a_k$ and $b_{l,m}$ are constants. Note that the $b$'s are not all independent and depend only on 2 real parameters. The argument based on the fundamental group for algebraic functions holds, in particular, the formula (7) for the path $\Gamma$.

As shown in an example below, if the coefficient of the highest order of $p$ in the Hamiltonian does not depend on the variable $q$, the action integral along $\gamma_i$ loop turns out to be 0 (see appendix B).

More specifically we will work with

$$H(p,q) = \frac{1}{2}(p^2+x^2) - \frac{1}{2}(p^2+x^2)^2 - 2x^2p^2, \tag{36}$$

where $x := 1-q^2$. The symmetry condition (1) is maintained. As seen in the phase space portrait drawn in figure 11, the system has two symmetric wells located at the positions $q = \pm 1$ respectively, and nonlinear resonance like equi-energy contours appear around each well.

In order to perform semiclassical analysis for the tunnelling splitting, as was done in the previous examples, we first examine the Riemann surface and the associated fundamental group. From the Hamiltoninan (36), we easily find

$$p(q) = \sqrt{\pm\frac{\sqrt{-8E+32x^4-8x^2+1}}{-2} - 3x^2 + \frac{1}{2}}. \tag{37}$$

The branch points are obtained by solving simultaneous algebraic equations

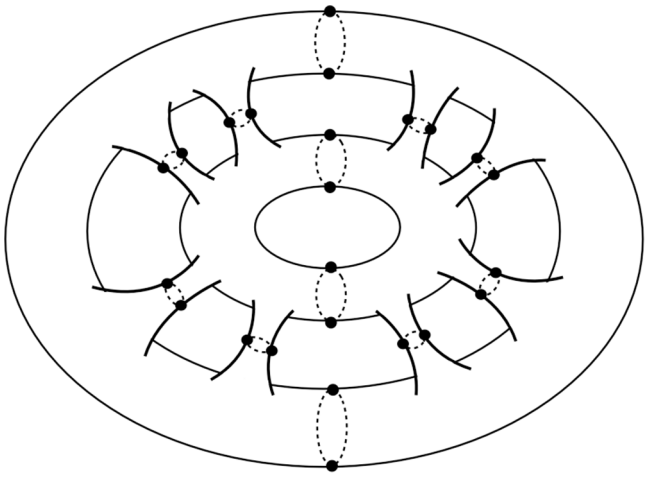

**Figure 12.** The Riemann surface of $p(q)$ for the Hamiltonian (36). The Riemann surface forms a 9-fold torus. The black dots and dashed curves are branch points and branch cuts, respectively.

$$\pm \frac{\sqrt{-8E + 32x^4 - 8x^2 + 1}}{-2} - 3x^2 + \frac{1}{2} = 0,$$
$$-8E + 32x^4 - 8x^2 + 1 = 0,$$

which provide 24 branch points in total. Each branch point is locally square-root type, thereby the corresponding Riemann surface $R$ has four leaves. Using the formula evaluating the genus, we find that the Riemann surface $R$ is homeomorphic to 9-fold torus with 28 small holes associated with 4 poles and 24 branch points. The Riemann surface is illustrated in figure 12. There are 9 $\alpha$- and $\beta$-loops together with 24 $\gamma$-loops associated with the branch points and 4 $\gamma$-loops with poles, each of which is attached in the corresponding leaf. From these observations, we have 45 independent action integrals in the semiclassical formula. However, as shown in appendix B, the action integrals for $\gamma$-loops for branch points are all zero, and the residues at the poles vanish. This fact simplifies the expression of action integrals as

$$S_\Gamma = S_{\Gamma_0} + \sum_{i=1}^{9} n_{\alpha_i} S_{\alpha_i} + \sum_{i=1}^{9} n_{\beta_i} S_{\beta_i}. \tag{38}$$

The next step is to single out the most dominant path out of all the candidates given above. Since $\mathrm{d}q = p\mathrm{d}t$ does not hold any more, we cannot *a priori* compare the different $\mathrm{Im}\, S$ even with an increasing $\mathrm{Im}\, \mathrm{d}t < 0$ and the usual heuristic selection argument may fail, as will be shown below.

## 8. Tunnelling splitting for the normal form Hamiltonian

In the following, we discuss the tunnelling splitting $\Delta E_n$ for the normal form Hamiltonian (36) based on the semiclassical analysis. Note however that the semiclassical analysis performed here will not fully be based on the semiclassical formula (3), and could be done only with a heuristic recipe. This is because, as shown below, that non-trivial situations actually arise from the handling of the Stokes phenomenon, so the selection of the most

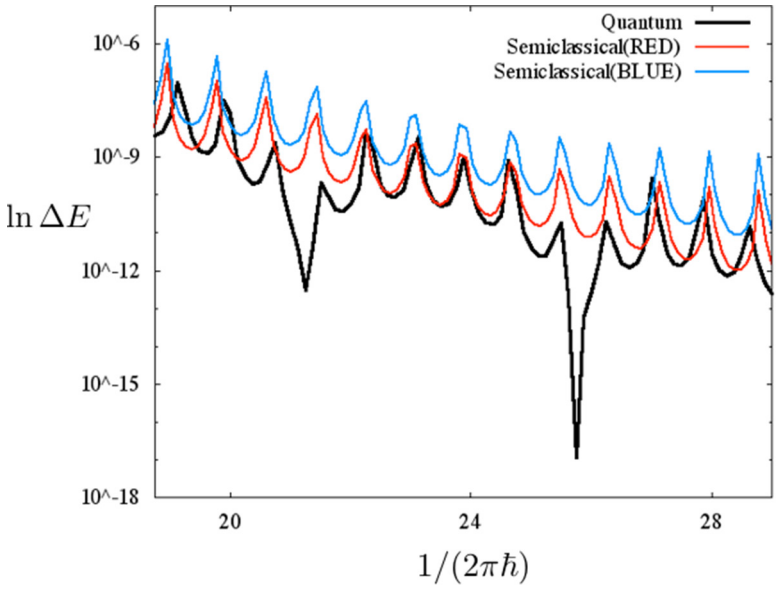


**Figure 13.** The tunnelling splitting $\Delta E_n = E_n^- - E_n^+$ as a function of $1/\hbar$. Here $E_n^+ \simeq E_n^- \simeq E = 6.19 \times 10^{-3}$. The black curve shows the numerical result obtained by direct calculation. The blue and red ones are obtained by applying the semiclassical formula (44), and the corresponding time paths are respectively shown in figure 16.

dominant complex path would be highly non-trivial. We focus on the tunnelling splitting $\Delta E_n = E_n^- - E_n^+$ for $E_n^+ \simeq E_n^- \simeq E$ below the barrier. Figure 13 plots $\Delta E_n$ as a function of $1/\hbar$ for $E = 6.19 \times 10^{-3}$.

In classical phase space, there appear congruent energy contour pairs in both sides of equi-energy contours, reflecting the symmetry with respect to the $q$-direction. For the energy satisfying $E \sim E_n^{\pm}$, there appear two closed energy contours in each side, which are shown in magenta curves in figure 14. Obviously, due to the symmetry, there are only two characteristic real periods $T_{\rm out}$ and $T_{\rm in}$ and two actions $S_{\rm out}$ and $S_{\rm in}$ associated with the outer and inner orbits respectively. The latter are connected via complex manifolds, which are shown in blue curves in figure 14, and outer periodic orbits in both sides are also connected via complex manifolds, drawn in green curves. Complex manifolds are obtained by integrating Hamiltonian equations of motion in the purely imaginary direction starting from each point of periodic orbits.

Following the argument developed in [15], we consider the time path in the complex plane for the orbit contributing to the semiclassical formula (3). The total elapsed time $T$ is written as

$$T \sim R(T) + \mathrm{i}T_{\rm in-out} + \mathrm{i}T_{\rm out-out} + \mathrm{i}T_{\rm in-out} + L(T). \tag{39}$$

where $\mathrm{i}T_{\rm in-out}$ is the time interval during which the complex orbit runs from the inner energy to the outer energy curve within the same well, shown in blue curves in figure 14. Similarly, $\mathrm{i}T_{\rm out-out}$ is the purely imaginary interval between the outer energy curve in the left side to another outer curve in the right side, shown in green curves in figure 14. $L(T)$ and $R(T)$ are sums of time intervals spent by the orbit moving in the inner and outer real energy curves, i.e.

$$L(T) = n_{\rm in}T_{\rm in} + n_{\rm out}T_{\rm out}, \tag{40}$$

$$R(T) = n'_{\rm in}T_{\rm in} + n'_{\rm out}T_{\rm out}, \tag{41}$$

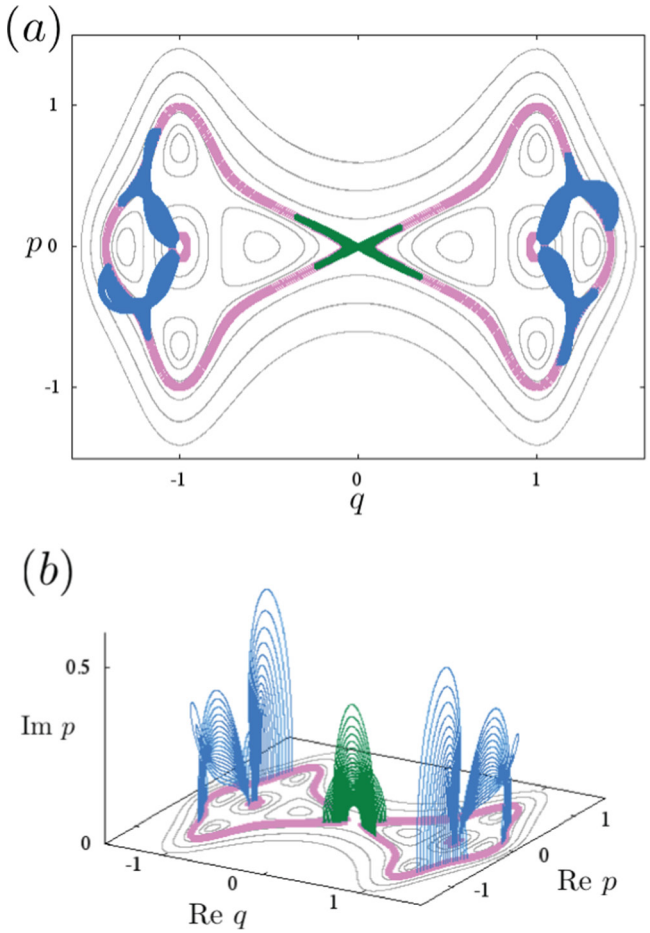


**Figure 14.** (a) Equi-energy contours for the Hamiltonian (36). The magenta curves show energy contours satisfying the condition $E \sim E_n^{\pm}$ where $E = 6.19 \times 10^{-3}$. The blue curves are projections onto the real plane of complex manifolds connecting inside and outside energy contours. The green one shows projection of complex manifolds connecting left and right outer energy contours. (b) The projection of each manifold onto $(\mathrm{Re}\, q, \mathrm{Re}\, p, \mathrm{Im}\, p)$ space.

where the winding numbers $n_{\mathrm{in}}, n_{\mathrm{out}}, n'_{\mathrm{in}}$ and $n'_{\mathrm{out}}$ are taken to be positive integers. A comment concerning $L(T)$ and $R(T)$ is in order. In [15], a fractional time interval $\tau$, or a residual time, was introduced for the time interval along the real direction as $\mathrm{Re}\, T = L(T) + R(T) - \tau$ in order to adjust the time interval in such a way that initial and final points are located at desired positions. However this residual time $\tau$ does not play any roles after taking the limit $\mathrm{Re}\, T \to \infty$ [15]. The corresponding action integral is then written as

$$\begin{aligned} S \sim\ & n_{\mathrm{in}} S_{\mathrm{in}} + \mathrm{i} S_{\mathrm{in-out}}/2 + n_{\mathrm{out}} S_{\mathrm{out}} \\ & + \mathrm{i} S_{\mathrm{out-out}}/2 \\ & + n'_{\mathrm{in}} S_{\mathrm{in}} + \mathrm{i} S_{\mathrm{in-out}}/2 + n'_{\mathrm{out}} S_{\mathrm{out}}. \end{aligned} \tag{42}$$

Here we focus only on the trajectories running on the complex manifolds connecting the real energy curves only once, as illustrated in figure 15. Hence, under the restrictions given in (40) and (41), the sum of contributions of such trajectories takes the form as

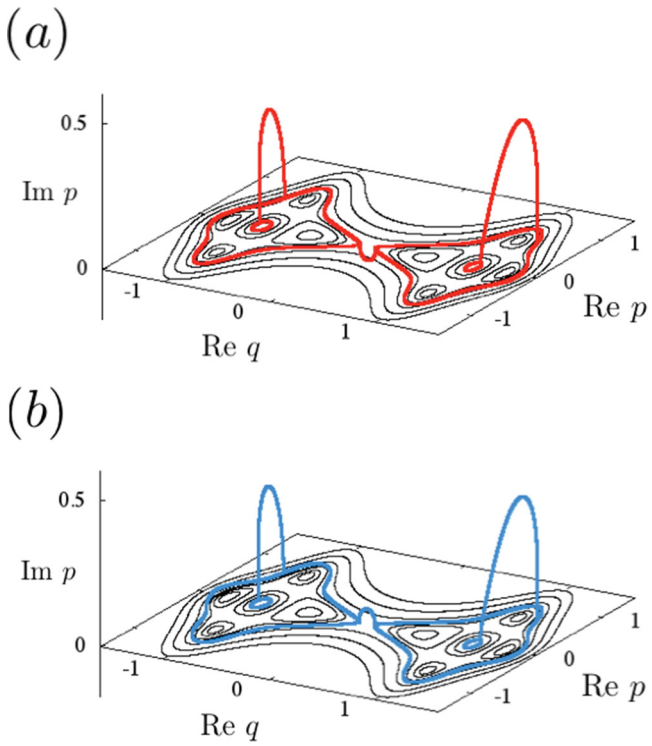


**Figure 15.** The projection of complex paths onto $(\mathrm{Re}\ q, \mathrm{Re}\ p, \mathrm{Im}\ p)$ space in the case (a) where the corresponding time path is taken as the red line in figure 16 and (b) where the blue path is taken, respectively. The energy for red and blue colored curves is given as $E = 6.19 \times 10^{-3}$.

$$\sum_{n_{\mathrm{in}}} \sum_{n'_{\mathrm{in}}} (-1)^{\mu+1} 4(n_{\mathrm{in}}+1)4(n'_{\mathrm{in}}+1) \mathrm{e}^{\mathrm{i}(n_{\mathrm{in}}S_{\mathrm{in}} + \mathrm{i}S_{\mathrm{in-out}}/2 + n_{\mathrm{out}}S_{\mathrm{out}})/\hbar} \times \mathrm{e}^{(-S_{\mathrm{out-out}}/2)/\hbar} \mathrm{e}^{\mathrm{i}(n'_{\mathrm{in}}S_{\mathrm{in}} + \mathrm{i}S_{\mathrm{in-out}}/2 + n'_{\mathrm{out}}S_{\mathrm{out}})/\hbar}. \tag{43}$$

Here the Maslov index is evaluated as $\mu = n_{\mathrm{in}} + n_{\mathrm{out}} + n'_{\mathrm{in}} + n'_{\mathrm{out}} + 7$. We may take the sums for $n_{\mathrm{in}}$ and $n'_{\mathrm{in}}$ separably, and each sum is the same as the one in the triple-well case in [15]. These lead us to the semiclassical expression for the tunnelling splitting

$$\Delta E_n \sim \frac{2\hbar}{T_{\mathrm{in}}} \left( \frac{\mathrm{e}^{-S_{\mathrm{in-out}}/(2\hbar)}}{\sin(((T_{\mathrm{out}}/T_{\mathrm{in}})S_{\mathrm{in}} - S_{\mathrm{out}})/(2\hbar))} \right)^2 \mathrm{e}^{-S_{\mathrm{out-out}}/2\hbar}. \tag{44}$$

Using this formula, we now demonstrate that a proper treatment of the Stokes phenomenon is crucial to discuss the tunnelling splitting of the normal form Hamiltonian within the semiclassical framework. In figure 13, we compare the splitting calculated using direct diagonalization with the ones obtained using the semiclassical formula (44). In the semiclassical calculation, we show the splittings evaluated using the complex path, which are drawn as red and blue zig–zag lines in the complex time plane (see figure 16). Note that both paths connect the left- and right wells and satisfy the boundary conditions necessary for the semiclassical formula.

As noticed from figure 16, the time path shown in blue satisfies the condition that $\mathrm{Im}\, T$ monotonically decreases whereas the path in red breaks the monotonicity. According to the criterion adopted in sections 4 and 5, the red-colored path should be dropped from the final

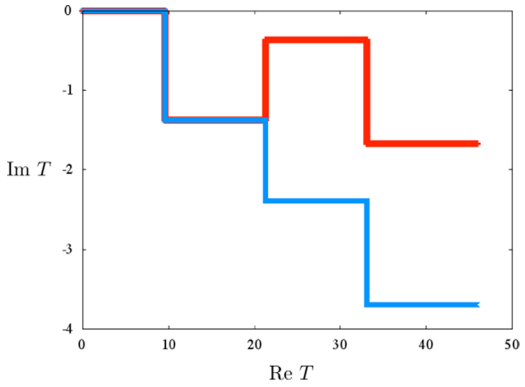


**Figure 16.** Complex time paths which are taken to test the semiclassical formula (see text). The imaginary time monotonically decreases in the blue path case while monotonicity condition is not satisfied in the red path case.

contribution because the path contains an interval in which $\mathrm{Im}\,T$ increases and expected to provide an exponentially exploding contribution which should be excluded from the final sum. However, as seen in figure 13, the curve based on the red-path contribution gives a larger slope as compared to the blue one, and shows better fitting to the exact plot. This result provides evidence implying that a naive criterion to treat the Stokes phenomenon does not work in the case studied here. The result also strongly suggests that exponentially decreasing solutions do not necessarily remain as contributions. This is counterintuitive in the conventional semiclassical argument as well.

## 9. Summary and discussion

In this paper we have investigated the topology of complex paths in one-dimensional systems to enumerate possible complex paths which contribute to the semiclassical sum formula for tunnelling splittings. Here Hamiltonian functions were assumed to be written as polynomials of the variables $p$ and $q$, thereby we could make use of knowledge on algebraic functions, especially the fundamental group for the Riemann surface. Since the action integral is the most important ingredient in the semiclassical formula, we examined the Riemann surface of the function $p(q)$ closely and showed that it has a finite number of leaves and homeomorphic to a multi-handled compact surface. The number of loops of the homology basis for the associated fundamental group turns out to be finite, reflecting the fact that the function $p(q)$ is algebraic.

To enumerate independent action integrals, it would be natural to consider independent elements in the fundamental group of the function $p(q)$. However this is not enough for our semiclassical analysis because the action integral is defined by the integration of $p(q)$ along an integration contour, so one has to take into account not only branch points generating the multivaluedness of the function $p(q)$, but also other singularities of $p(q)$ with non-zero residues. Such singularities indeed appear in the Riemann surface as divergent points of $p(q)$.

As model systems, we here studied the double- and triple-well potential systems, together with the normal form Hamiltonians as well. For the former two cases, we have obtained the complete list of the possible complex paths based on the idea employing the fundamental group. As a bi-product out of such a systematic treatment, we derived action relations involving the residue contribution from divergent points of $p(q)$. Note that the relation for the double-well case has already been obtained in [32], but its origin could more simply be

understood through the fundamental group argument. In the case of the double-well potential system for instance, we usually consider the quantization condition for each well independently since the equi-energy surfaces in left- and right-side wells are classically disjoined. However our analysis exploring the topology of the whole complex equi-energy surfaces has unveiled that quantization conditions in left and right wells are linked through the action integral associated with infinity of the Riemann surface. Similar action relations were similarly derived in the triple-well potential system, and they lead to simultaneous quantization of left- and right-wells if the potential is symmetric.

In performing the semiclassical analysis, it is not sufficient to enumerate the complex paths satisfying the boundary conditions required in the semiclassical formula. Since the semiclassical formula is obtained by applying the saddle point method, one needs to handle the Stokes phenomenon in an appropriate manner. In the semiclassical arguments for tunnelling splittings so far, this issue has not been discussed seriously even in one-dimensional situations. The most typical approach would be just to remove exponentially exploding solutions, which is based only on a rather naive speculation in analogy with a treatment of the Airy function. The well-known instanton theory and its variants applied to more general situations have adopted essentially the same strategy. However, as shown in the present paper, the possible classical actions are expressed as a linear combination of elements of the fundamental group together with contributions from divergent singularities. This brings infinitely many possible candidates, and infinitely many exploding solutions are necessarily contained among them. As a result, it becomes a crucial step to deal with the Stokes phenomenon properly. This is entirely beyond the scope of this paper, and here we only tested the most conventional prescription. For the double- and triple-well potential systems, we extracted the complex paths remaining as semiclassical contributions in such a way that the imaginary direction of the corresponding time path should be negative, which guarantees the monotonicity of imaginary action of complex paths. We confirmed that the results were both consistent with known results.

In the normal form Hamiltonian case, we could also find all the possible complex paths based on the fundamental group because the Hamiltonian is also given as a polynomial function. However, a naive treatment of the Stokes phenomenon was shown to break down. In particular, we demonstrated that there is a situation where even exponentially decaying contributions should be dropped, which is one piece of evidence suggesting that the Stokes phenomenon for the normal form Hamiltonian systems must be highly non-trivial [36].

Our motivation for studying the normal form Hamiltonian was to promote our understanding of the so-called resonance-assisted tunnelling as was done in [20]. As stressed in this paper, equi-energy contours of the normal form Hamiltonian apparently look like patterns typically appearing in Poincaré sections of two-dimensional nearly integrable system, but nonlinear resonance like structures in one-dimensional systems are not caused by nonlinear resonances. It would therefore be unreasonable to explain the mechanism of tunnelling occurring in two-dimensional nonintegrable systems based on one-dimensional systems even though apparent similarity exists in their phase space patterns.

Even if one concedes that the normal form Hamiltonian could somehow serve as an analogous model to the system with nonlinear resonances, the analysis based on the fundamental group tells us that what is relevant is the topology of the Riemann surface, which is entirely controlled by the branch points of the function $p(q)$. This implies that instanton in the conventional sense might play only a relative role. The understanding of instanton has been updated from the perspective of the relevance of the Riemann sheet structure, which is based on a similar spirit as our present arguments [37, 38].

One important message out of this paper would be that one does not need to consider the time path any more and has only to focus on the function $p(q)$. Instanton has a long history

and the idea using the complex time plane has been and still must be dominant, but this would not be a right strategy as discussed in the present paper and [37, 38] as well. What we need is information on the function $p(q)$, not the complex structure of functions $q(t)$ and $p(t)$, so analyzing the fundamental group for the Riemann surface of $p(q)$ would become unavoidable.

## Acknowledgments

The authors are very grateful to Masanori Kobayashi for many valuable comments on the fundamental group for algebraic functions. This work has been supported by JSPS KAKENHI Grant Numbers 25400405 and 15H03701.

## Appendix A. Semiclassical formula of tunnel splittings

In this appendix, we briefly sketch the derivation of the formula (3), following [15]. Let $|\phi_n^{\pm}\rangle$ be symmetric and asymmetric quasi-degenerated states for a Hamiltonian commuting with the parity operator $\hat{S}$ such that $\hat{S}^2 = 1$. The eigenstates of $\hat{H}$ can be classified according to their parity,

$$\hat{S}|\phi_n^{\pm}\rangle \stackrel{\text{def}}{=} \pm|\phi_n^{\pm}\rangle. \tag{A.1}$$

The spectral decomposition of the evolution operator after a time $T$ writes

$$\hat{U}(T) = \sum_n (\mathrm{e}^{\frac{1}{\mathrm{i}\hbar}E_n^+ T}|\phi_n^+\rangle\langle\phi_n^+| + \mathrm{e}^{\frac{1}{\mathrm{i}\hbar}E_n^- T}|\phi_n^-\rangle\langle\phi_n^-|). \tag{A.2}$$

To discuss the tunnelling splitting between the states $|\phi_n^+\rangle$ and $|\phi_n^-\rangle$, we further define the projection operator

$$\hat{\Pi}_n \stackrel{\text{def}}{=} |\phi_n^+\rangle\langle\phi_n^+| + |\phi_n^-\rangle\langle\phi_n^-|. \tag{A.3}$$

and we have

$$\mathrm{Tr}(\hat{\Pi}_n\hat{U}) = \sum_m \langle\phi_m^{\pm}|\hat{\Pi}_n\hat{U}|\phi_m^{\pm}\rangle = \mathrm{e}^{-\frac{\mathrm{i}}{\hbar}E_n^+ T} + \mathrm{e}^{-\frac{\mathrm{i}}{\hbar}E_n^- T}, \tag{A.4}$$

$$\mathrm{Tr}(\hat{S}\hat{\Pi}_n\hat{U}) = \mathrm{e}^{-\frac{\mathrm{i}}{\hbar}E_n^+ T} - \mathrm{e}^{-\frac{\mathrm{i}}{\hbar}E_n^- T}. \tag{A.5}$$

We then obtain

$$\frac{\mathrm{Tr}(\hat{S}\hat{\Pi}_n\hat{U})}{\mathrm{Tr}(\hat{\Pi}_n\hat{U})} = \mathrm{i}\tan(\frac{\Delta E_n}{2\hbar}T). \tag{A.6}$$

where $\Delta E_n = E_n^- - E_n^+$. If the condition

$$\frac{|T|\Delta E_n}{2\hbar} \ll 1 \tag{A.7}$$

is satisfied, the tunnelling splitting $\Delta E_n$ can be explicitly written as

$$\Delta E_n \sim \frac{2\hbar}{\mathrm{i}T}\frac{\mathrm{Tr}(\hat{S}\hat{\Pi}_n\hat{U})}{\mathrm{Tr}(\hat{\Pi}_n\hat{U})}. \tag{A.8}$$

We now rewrite the right-hand side of (A.8) in the path integral form. Introducing the quasi-mode $|\Phi_n\rangle \stackrel{\text{def}}{=} (|\phi_n^+\rangle + |\phi_n^-\rangle)/\sqrt{2}$, the projection operator is expressed as

$$|\phi_n^+\rangle\langle\phi_n^+| + |\phi_n^-\rangle\langle\phi_n^-| = |\Phi_n\rangle\langle\Phi_n| + \hat{S}|\Phi_n\rangle\langle\Phi_n|\hat{S}. \tag{A.9}$$

Let $\Phi_n^{sc}(q)$ be WKB approximation of $\Phi_n(q)$ [39, 40], which is localized on the energy curve satisfying $E \sim E^{\pm}$, then the numerator and denominator of the formula (A.8) are semiclassically evaluated as

$$2\int \mathrm{d}q\mathrm{d}q' \Phi_n^{sc}(q)(\Phi_n^{sc}(q'))^* G(\eta q', q; T), \tag{A.10}$$

where $G(\eta q', q; T)$ represents the Van Vleck-Gutzwiller propagator

$$G(\eta q', q; T) = \sum_{\gamma}(-1)^{k_\gamma}\sqrt{\det\left(\frac{\mathrm{i}}{2\pi\hbar}\frac{\partial^2 S_\gamma}{\partial q_f \partial q_i}\right)}\mathrm{e}^{\frac{\mathrm{i}}{\hbar}S_\gamma(\eta q', q; T)}. \tag{A.11}$$

Here $\eta = -1$ for the numerator and $\eta = +1$ for the denominator of the formula (A.8), respectively. The index $k_\gamma$ denotes the number of conjugation points along the trajectory $\gamma$.

We further evaluate the integral (A.10) again using the saddle point approximation, which requires the condition

$$\lim_{q_f \to \eta q_i} \frac{\delta S_\gamma}{\delta q_i} = \frac{\partial S_\gamma}{\partial q_i} + \frac{\partial q_f}{\partial q_i}\frac{\partial S_\gamma}{\partial q_f} = 0. \tag{A.12}$$

Then the generating relations

$$\frac{\partial S_\gamma}{\partial q_i} = -p_i, \qquad \frac{\partial S_\gamma}{\partial q_f} = \eta p_f, \tag{A.13}$$

leads to the condition

$$p_f = \eta p_i \tag{A.14}$$

for each $\eta$. By taking the trace of integral (A.10), the classical paths contributing to the final semiclassical sum should altogether satisfy the conditions $E \sim E_n^{\pm}$, $q_f = \eta q_i$ and $p_f = \eta p_i$. In section 2, $q_f$ and $q_i$ are expressed as $q(T)$ and $q(0)$, respectively (same as for $p$). After calculating the prefactor in evaluating the integral (A.10) (see details in [15]), we finally reach the formula (3).

## Appendix B. Integral along $\gamma$ loops

In this appendix we calculate the integral whose integration contour encircles a single branch point $q_i$ of the function $p(q)$. In the text, such a loop is called the $\gamma_i$ loop.

Branch points of the algebraic function are algebraic singularities around which $p$ has the Puiseux expansion in the following form

$$p(q) = \sum_{n=s}^{\infty} c_n (q - q_i)^{\frac{n}{w}}, \qquad (s > -\infty) \tag{B.1}$$

where $w$ is a positive number.

Putting $t = (q - q_i)^{1/w}$, we evaluate each term of the expansion as

$$\frac{1}{2\pi i}\int_C (q - q_i)^{\frac{n}{w}}\mathrm{d}q = \frac{w}{2\pi\mathrm{i}}\oint t^{n+w-1}\mathrm{d}t = \begin{cases} w & \text{if } n + w = 0 \\ 0 & \text{otherwise,} \end{cases} \tag{B.2}$$

where $C$ is a closed curve circling around the point $q = q_i$ $w$ times.

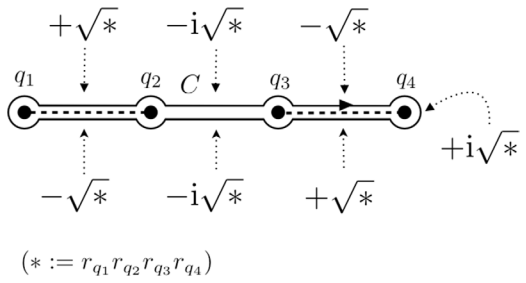


**Figure C1.** The integration contour $C$ and the phase of $p(q)$ at each position. The black dots are branch points. The dash lines represent the branch cuts.

For a Hamiltonian of the form $H = p^2/2 + V(q)$ where $V(q)$ is a polynomial function of $q$, the function $p(q)$ does not contain negative order terms in the corresponding Puiseux series. Therefore the action integrals for the $\gamma_i$ loops all vanish. For the normal form Hamiltonian (35), if the condition $2k > m$ holds, the $\gamma_i$ contributions are all zero as well since $p(q)$ does not contain negative order terms in the Puiseux series. On the other hand, for $2k \leqslant m$, the coefficient for the highest order of $p$ contains the variable $q$, resulting in a non-zero contribution from $\gamma_i$ loops.

## Appendix C. The action relation and the residue at infinity

In this appendix, we provide an explicit derivation of action relations. The following calculations can easily be generalized to the multi-well potential systems. We here present double- and triple-well cases as examples.

### *C.1. Double-well case*

Let us consider the Hamiltonian:

$$H = \frac{p^2}{2} + V(q), \tag{C.1}$$

where $V(q) = E + (q - q_1)(q - q_2)(q - q_3)(q - q_4)$. Branch points of $p(q)$ at the energy $E$ are located at $q = q_i$ $(1 \leqslant i \leqslant 4)$. Let $C$ be a closed curve rotating clockwise around all branch points (figure C1). The loop $C$ is homotopic to the loop around infinity on the Riemann sphere, so the integration along this loop is equal to the residue of infinity. We calculate the residue at $q = +\infty$ as follows. Introducing a new coordinate $q = 1/\eta$, we find

$$\begin{aligned}\oint_{\Gamma^{(\infty)}} p(q)\mathrm{d}q &= \oint \frac{1}{\eta^2}\sqrt{-W(\eta)}\left(\frac{-1}{\eta^2}\right)\mathrm{d}\eta \\ &= \oint \frac{-1}{\eta^4}\left(\sum_k C_k \eta^k\right)\mathrm{d}\eta,\end{aligned}$$

where $W(\eta) := 2(1 - q_1\eta)(1 - q_2\eta)(1 - q_3\eta)(1 - q_4\eta)$, and $C_k$ $(k \geqslant 0)$ are coefficients of the Taylor expansion of $\sqrt{-W(\eta)}$. $\Gamma^{(\infty)}$ denotes a single loop encircling $\eta = 0$. For the integration over $\eta$, the loop rotates anticlockwise around $\eta = 0$, and the residue is evaluated as $-2\pi\mathrm{i}C_3$. An explicit form of $C_3$ is

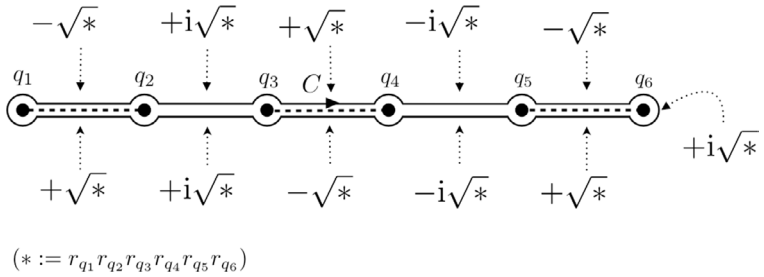


**Figure C2.** The integration contour $C$ and the phase of $p(q)$ at each position. The black dots are branch points. The dash lines represent the branch cuts.

$$C_3 = \mathrm{i}\Big(\frac{1}{4}(q_1+q_2+q_3+q_4)(q_1q_2+q_1q_3+q_2q_3 - \frac{1}{4}(q_1+q_2+q_3+q_4)^2 + q_1q_4+q_2q_4+q_3q_4) + \frac{1}{2}(-q_1q_2q_3 - q_1q_2q_4 - q_1q_3q_4 - q_2q_3q_4)\Big).$$

Hence we obtain $S^{(\infty)} := \oint_{\Gamma(\infty)} p(q)\mathrm{d}q = -2\pi\mathrm{i}C_3$.

On the other hand, we evaluate the same integral by taking the integration along the real axis. We introduce new coordinates $r_{q_i}$ and $\theta_{q_i}$ as $r_{q_i}\mathrm{e}^{\mathrm{i}\theta_{q_i}} := q - q_i$ $(1 \leqslant i \leqslant 4)$. Here we have to take a close look at the phase of the function $p(q)$ and the upper limit of the integration. If we take the phase as $p(q) = \mathrm{i}\sqrt{r_{q_1}r_{q_2}r_{q_3}r_{q_4}}$, the upper limit should satisfy the condition $q_4 < q$ in order that the phase of $p(q)$ is consistent with the residue calculation at infinity, as shown in figure C1. We therefore obtain

$$\begin{aligned}\oint_C p(q)\mathrm{d}q &= 2\int_{q_1}^{q_2} p\mathrm{d}q - 2\int_{q_3}^{q_4} p\mathrm{d}q \\ &= S_L - S_R.\end{aligned} \tag{C.2}$$

Finally we get the relation (15)

$$S^{(\infty)} = \oint_{\Gamma(\infty)} p(q)\mathrm{d}q = \oint_C p(q)\mathrm{d}q = S_L - S_R. \tag{C.3}$$

### *C.2. Triple-well case*

For the triple well case where $V(q) = E + (q-q_1)(q-q_2)(q-q_3)(q-q_4)(q-q_5)(q-q_6)$, we find

$$\begin{aligned}\oint_{\Gamma(\infty)} p(q)\mathrm{d}q &= \oint \frac{1}{\eta^3}\sqrt{-W(\eta)}\Big(\frac{-1}{\eta^2}\Big)\mathrm{d}\eta \\ &= \oint \frac{-1}{\eta^5}\left(\sum_k C_k\eta^k\right)\mathrm{d}\eta.\end{aligned}$$

Here $W(\eta) := 2(1-\eta q_1)(1-\eta q_2)(1-\eta q_3)(1-\eta q_4)(1-\eta q_5)(1-\eta q_6)$, and $C_k$ $(k \geqslant 0)$ are coefficients of the Taylor expansion of $\sqrt{-W(\eta)}$. The residue is evaluated as $-2\pi\mathrm{i}C_4$. Hence we obtain $S^{(\infty)} := \oint_{\Gamma(\infty)} p(q)\mathrm{d}q = -2\pi\mathrm{i}C_4$.

On the other hand, we calculate the same integral along the real axis. As shown in figure C2, we choose a closed curve $C$ rotating clockwise around all branch points, and introduce new coordinates $r_{q_i}$ and $\theta_{q_i}$ as $r_{q_i}\mathrm{e}^{\mathrm{i}\theta_{q_i}} := q - q_i$ $(1 \leqslant i \leqslant 6)$. If we take the phase as $p(q) = \mathrm{i}\sqrt{r_{q_1}r_{q_2}r_{q_3}r_{q_4}r_{q_5}r_{q_6}}$, the upper limit should satisfy the condition $q_6 < q$ in order that the phase of $p(q)$ should be consistent with the residue calculation at infinity, as shown in figure C2. Then we obtain

$$\begin{aligned}\oint_C p(q)\mathrm{d}q &= -2\int_{q_1}^{q_2} p\mathrm{d}q + 2\int_{q_3}^{q_4} p\mathrm{d}q - 2\int_{q_5}^{q_6} p\mathrm{d}q \\ &= -S_L + S_C - S_R. \end{aligned} \tag{C.4}$$

Finally we reach the relation (28)

$$S^{(\infty)} = -S_L + S_C - S_R. \tag{C.5}$$

## ORCID iDs

Hiromitsu Harada https://orcid.org/0000-0002-3832-8410
Akira Shudo https://orcid.org/0000-0001-9443-9054

## References

[1] Coleman S 1985 *Aspects of Symmetry* (*Selected Erice Lectures*) (Cambridge: Cambridge University Press)
[2] Freed K F 1972 *J. Chem. Phys.* **56** 692
[3] George T F and Miller W H 1972 *J. Chem. Phys.* **56** 5722
[4] Miller W H 1974 *Adv. Chem. Phys.* **25** 69
[5] Weiss U and Haeffner W 1983 *Phys. Rev.* D **27** 2916
[6] Carlitz R D and Nicole D A 1985 *Ann. Phys., NY* **164** 411
[7] Ilgenfritz E M and Perlt H 1992 *J. Phys. A: Math. Gen.* **25** 5729
[8] Creagh S C and Whelan N D 1999 *Ann. Phys., NY* **272** 196
[9] Bohigas O, Tomsovic S and Ullmo D 1993 *Phys. Rep.* **223** 43
[10] Creagh S C 1988 *Tunneling in Complex Systems* ed S Tomsovic (Singapore: World Scientific) p 35
[11] Keshavamurthy S and Schlagheck P 2011 *Dynamical Tunneling: Theory and Experiment* (Boca Raton, FL: CRC Press)
[12] Landau L D and Lifshitz E M 1977 *Quantum Mechanics (Non-relativistic Theory), Course of Theoretical Physics* vol 3, 3rd edn (Oxford: Pergamon)
[13] Connor J N L, Uzer T, Marcus R A and Smith A D 1984 *J. Chem. Phys.* **80** 5095
[14] Garg A 2000 *Am. J. Phys.* **68** 430
[15] Le Deunff J and Mouchet A 2010 *Phys. Rev.* E **81** 046205
[16] Maslov V P and Fedoriuk M V 1981 *Semi-Classical Approximation in Quantum Mechanics* (Boston: Reidel)
[17] Voros A 1983 *Ann. Inst. Henri Poincare* A **39** 211
[18] Delabaere E, Dillinger H and Pham F 1997 *J. Math. Phys.* **37** 6126
[19] Kawai T and Takei Y 2006 *Algebraic Analysis of Singular Perturbation Theory* (*Translations of Mathematical Monographs*) (Providence, RI: American Mathematical Society)
[20] Le Deunff J, Mouchet A and Schlagheck P 2013 *Phys. Rev.* E **88** 042927
[21] Brodier O, Schlagheck P and Ullmo D 2002 *Ann. Phys.* **300** 88
[22] Shudo A, Ishii Y and Ikeda K S 2008 *J. Phys. A: Math. Theor.* **42** 265101
Shudo A, Ishii Y and Ikeda K S 2009 *J. Phys. A: Math. Theor.* **42** 265102
[23] Shudo A and Ikeda K S 2011 *Dynamical Tunneling* ed S Keshavamurthy and P Schlagheck (Boca Raton, FL: CRC Press) ch 7 p 139
[24] Takahashi K and Ikeda K S 2000 *Ann. Phys.* **283** 94

[25] Takahashi K and Ikeda K S 2001 *Found. Phys.* **31** 177
[26] Takahashi K, Yoshimoto A and Ikeda K S 2002 *Phys. Lett.* A **297** 370
[27] Honda N, Kawai T and Takei Y 2015 *Virtual Turning Points* (*Springer Briefs in Mathematical Physics*) (New York: Springer)
[28] Schlag W 2014 *A Course in Complex Analysis and Riemann Surfaces, Graduate Studies in Mathematics* vol 154 (Providence, RI: American Mathematical Society)
[29] Kosniowski C 1980 *A First Course in Algebraic Topology* (Cambridge: Cambridge University Press)
[30] Bohm D 1951 *Quantum Theory* (Englewood Cliffs, NJ: Prentice Hall)
[31] Schlagheck P, Mouchet A and Ullmo D 2011 *Dynamical Tunneling: Theory and Experimental* (Boca Raton, FL: CRC Press) ch 8
[32] Khuat-duy D and Leboeuf P 1993 *Appl. Phys. Lett.* **63** 1903
[33] Farkas H M and Kra I 1980 *Riemann Surfaces* (New York: Springer)
[34] Brodier O, Schlagheck P and Ullmo D 2001 *Phys. Rev. Lett.* **87** 064101
[35] Arnold V I 1978 *Mathematical Methods of Classical Mechanics* (New York: Springer)
[36] Shudo A and Ikeda K S 2016 *Nonlinearity* **29** 375
[37] Gulden T, Janas M, Koroteev P and Kamenev A 2013 *J. Exp. Theor. Phys.* **117** 517–37
[38] Gulden T, Janas M and Kamenev A 2015 *J. Phys. A: Math. Theor.* **48** 075304
[39] Keller J B 1958 *Ann. Phys., NY* **4** 180
[40] Percival I C 1977 *Adv. Chem. Phys.* **36** 1
[41] Harrell E M 1978 *Commun. Math. Phys.* **60** 73–95
[42] Davies E B 1982 *Commun. Math. Phys.* **85** 471–9
[43] Simon B 1983 *Bull. Am. Math. Soc.* **8** 323–6
[44] Simon B 1984 *Ann. Math.* **120** 89–118
[45] Helffer B and Sjöstrand J 1984 *Commun. PDE* **9** 337–408
[46] Helffer B and Sjöstrand J 1985 *J. Équ. Dérivées Part.* **2** 1–38 (in French) (www.numdam.org/item?id=JEDP_1985___2_A2_0+)
[47] Helffer B and Sjöstrand J 1986 *Mém. Soc. Math.* **114** 1–228 (in French) (www.numdam.org/item?id=MSMF_1986_2_24-25__1_0+)
[48] Helffer B and Sjöstrand J 1987 *Ann. Scuola Norm. Super. Pisa* **14** 625–57 (in French)
[49] Dobrokhotov Yu S, Kolokoltsov V N and Maslov V P 1991 *Theor. Math. Phys.* **87** 561–99 (Engl. transl.)
Dobrokhotov Yu S, Kolokoltsov V N and Maslov V P 1991 *Teor. Mat. Fiz.* **87** 323–75 (in Russian)
[50] Dobrokhotov Yu S and Kolokoltsov V N 1993 *Theor. Math. Phys.* **94** 300–5 (Engl. transl.)
Dobrokhotov Yu S and Kolokoltsov V N 1993 *Teor. Mat. Fiz.* **94** 426–34 (in Russian)
[51] Martinez A 1987 *J. Math. Pures Appl.* **66** 195–215 (in French)
[52] Martinez A 1988 *Bull. Soc. Math. France* **116** 199–229 (in French)
[53] Sordoni V 1997 *J. Math. Phys.* **38** 770–95